Iron Loss Analysis of Mn–Zn Ferrite Cores

Hideo Saotome, *Member, IEEE,* and Yo Sakaki, *Member, IEEE*

Abstract—**Iron loss measurements of Mn–Zn ferrite cores up to the megahertz range are reported. Taking the dc magnetic hysteresis, the eddy, and displacement currents into account, magnetic and electric field distributions in the cores are computed with the cylindrical coordinates and Bessel functions. The computed iron loss due to the magnetic and electric fields is compared with the experimental value at different exciting frequencies. It is noted that the computed iron loss becomes considerably smaller than the experimental at high frequencies. In order to explain the difference between the computed and experimental iron losses, a new magnetic field component yielding a dynamic magnetic loss is assumed and added to the magnetic field intensity of the dc magnetic hysteresis. This assumption is verified by evaluating the iron losses in different size cores composed of the same ferrite material. Displacement current distribution in a ferrite core depends on the cross-sectional area of the magnetic flux path, which brings about the dependence of the frequency characteristics of the iron loss upon core size.**

I. Introduction

FERRITES are used in high-frequency and high-speed switching circuits because their eddy current losses are considerably smaller than those of metallic magnetic materials. In soft ferrites, there are two major groups, i.e., Mn–Zn and Ni–Zn ferrites. Their electromagnetic characteristics are different: compared with Ni–Zn ferrites, Mn–Zn ferrites have relatively low resistivity, but large permeability. Therefore, Mn–Zn ferrites are used in applications up to the megahertz range.

Previous studies analyzed the iron loss of metallic materials by focusing on the eddy current loss in a uniformly distributed magnetic field [1], or by considering the magnetic domain structure [2]. On the other hand, recent studies of metallic materials suggested a loss parameter which expresses, in a lump, both the dc magnetic hysteresis and eddy current losses in the metallic layers of a laminated core [3], [4]. A similar parameter has been applied to the iron loss analysis for ferrite materials [5], [6]. As for ferrites, iron loss dependence upon the magnetic field intensity and the exciting frequency up to 1 MHz was analyzed experimentally by using the magnetic domain structure [7]. In the previous studies of ferrites, Hayano *et al.* considered magnetic field distribution in a core [5]; however, the obtained magnetic fields were uniform because the exciting frequencies were under 20 kHz. Sato and Sakaki carried out iron loss measurement up to 500 kHz, in which the magnetic field was assumed to be uniform in its analysis [6]. Ferrites have dielectric characteristics [8], [9] in addition to their magnetic and ohmic characteristics. However, the magnetic loss, the eddy, and displacement current losses are not separately treated in the analyses of [5] and [6]. Sakaki *et al.* took into account the displacement current in a ferrite core [10]; however, the computed frequency characteristics of the iron loss were smaller than the experimental results, which suggests that another loss factor, in addition to the dc magnetic hysteresis, the eddy, and displacement currents, exists in the core.

We carried out iron loss measurement of Mn–Zn ferrite cores up to the megahertz range, and computed frequency characteristics of the iron loss by taking the dc magnetic hysteresis, the eddy, and displacement currents into account. In order to compute the iron loss, we obtained the magnetic and electric field distributions in the cores from the governing equations derived from Maxwell's equations. A comparison between the computed and experimental results leads to the assumption of a dynamic magnetic loss parameter. This assumption is justified by the agreement of the frequency characteristics of the computed and experimental iron losses in different size cores composed of the same Mn–Zn ferrite material. Moreover, this paper shows that the core dimension dependence of iron loss density in ferrites [11] is caused by the difference of displacement current distribution in cores of different size.

II. Formulation of the Iron Loss in the Electromagnetic Field

Using a toroidal-shaped ferrite core model having a circular cross section shown in Fig. 1, we take into account and assume the following items in iron loss analysis:

1) The magnetic and electric field distributions in the core cross section. However, the leakage fluxes are not considered.

2) The dc magnetic hysteresis loss.

3) The eddy current loss due to the conductivity of the core body.

4) The permittivity of the core body and the ohmic losses in grains due to the displacement currents flowing in grain boundary regions.

5) The amplitude of the magnetic flux density in the core is under its saturation induction.

6) The exciting current waveform is sinusoidal, and the steady-state iron loss is obtained from the steady-state electromagnetic field distribution in the core.

From 1), the magnetic field intensity H and the magnetic flux density B only have the z component shown in

Manuscript received April 21, 1995; revised March 11, 1996.

The authors are with Department of Electrical and Electronics Engineering, Chiba University, 1-33 Yayoi, Inage, Chiba 263, Japan.

Publisher Item Identifier S 0018-9464(97)00127-1.

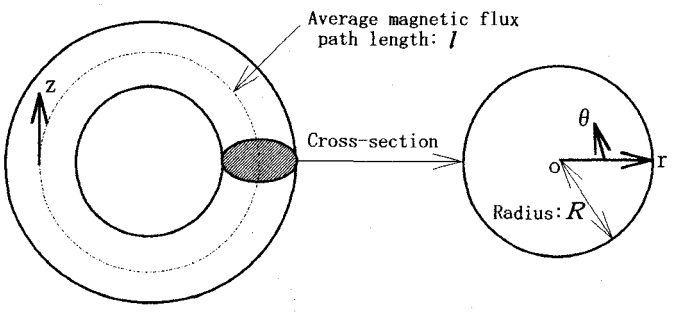

Fig. 1. Cylindrical coordinate system for analyzing the iron loss in a toroidal core.

Fig. 1. Similarly, the electric field intensity E and the dielectric flux density D are in the θ direction of Fig. 1. From 5) and 6), H, B, E, and D can be treated as phasors having effective values. The application of Maxwell's equations in the cylindrical coordinate system of Fig. 1 provides the governing equations for H and E with the angular frequency of the exciting current ω and $j = \sqrt{-1}$:

$$\frac{\partial^2 H}{\partial r^2} + \frac{1}{r}\frac{\partial H}{\partial r} + \omega\mu(\omega\epsilon - j\sigma)H = 0 \quad (1)$$

$$\frac{\partial^2 E}{\partial r^2} + \frac{1}{r}\frac{\partial E}{\partial r} + \left\{\omega\mu(\omega\epsilon - j\sigma) - \frac{1}{r^2}\right\}E = 0 \quad (2)$$

where σ, μ, and ϵ denote the conductivity, permeability, and permittivity of the ferrite core shown in Fig. 1, respectively. In order to take into account the loss caused by H and B, the permeability μ is regarded as a complex number. Similarly, ϵ is also treated as a complex permittivity which expresses the loss caused by E and D. Dielectric losses might occur in grain boundary regions. However, more dominant losses are assumed to occur in grains by the currents flowing from the grain boundary regions where they are displacement currents. In this paper, the ohmic losses in grains caused by the displacement currents are expressed by ϵ for convenience, and they are distinguished from the conventional eddy current losses owing to the dc conductivity σ of the core body. The dielectric losses in grain boundaries are also included in ϵ because grains and grain boundary regions are assumed to be connected in series for the displacement currents.

Let us assume the magnetic field intensity H_R on the circular contour $r = R$ in Fig. 1. In the area of $r < R$, the magnetomotive forces are affected not only by the exciting current, but also by the eddy and displacement currents. However, on the contour $r = R$, the magnetic field intensity H_R is determined only by the exciting current when the number of exciting coil turns and the magnetic flux path length are known. With the zeroth-order Bessel function of the first kind J_0, the boundary condition H_R gives the solution for (1):

$$H(r) = H_R \frac{J_0(kr)}{J_0(kR)} \quad (3)$$

where

$$k = \sqrt{\omega\mu(\omega\epsilon - j\sigma)}. \quad (4)$$

Equation (3) directly gives the electric field distribution $E(r)$ in the core by means of the surface integral of $\nabla \times E = -j\omega B$:

$$E(r) = -\frac{j\omega}{r}\int_0^r \mu H(r')\, r'\, dr' \quad (5)$$

because (1) is obtained by taking the electric field distribution into account. On the other hand, imposing the boundary condition at $r = R$,

$$E(R) = -\frac{j\omega}{R}\int_0^R \mu H(r)\, r\, dr \equiv -\frac{j\omega\Phi}{2\pi R}, \quad (6)$$

on (2) gives the solution

$$E(r) = -\frac{j\omega\Phi}{2\pi R}\frac{J_1(kr)}{J_1(kR)} \quad (7)$$

where Φ is the magnetic flux phasor having the effective value of the total magnetic flux in the core and J_1 is the first-order Bessel function of the first kind.

The eddy current loss P_E due to the conductivity σ of the core body having volume V is given by the volume integral

$$P_E = \int_V \sigma E(r)^2\, d\tau = 2\pi l\sigma \int_0^R E(r)^2\, r\, dr \quad (8)$$

where l denotes the average magnetic flux path length of the core shown in Fig. 1. Similarly, we have the magnetic and dielectric losses P_M and P_D as follows:

$$P_M = \int_V \tfrac{1}{2}\left[H(r)\left\{\overline{j\omega B(r)}\right\} + \overline{H(r)}\left\{j\omega B(r)\right\}\right] d\tau$$

$$= \pi l \int_0^R \left[H(r)\left\{\overline{j\omega B(r)}\right\} + \overline{H(r)}\left\{j\omega B(r)\right\}\right] r\, dr \quad (9)$$

$$P_D = \int_V \tfrac{1}{2}\left[E(r)\left\{\overline{j\omega D(r)}\right\} + \overline{E(r)}\left\{j\omega D(r)\right\}\right] d\tau$$

$$= \pi l \int_0^R \left[E(r)\left\{\overline{j\omega D(r)}\right\} + \overline{E(r)}\left\{j\omega D(r)\right\}\right] r\, dr \quad (10)$$

where the overbar denotes a conjugate complex number, and $B(r)$ and $D(r)$ are, respectively, obtained by multiplying (3) and (7) by μ and ϵ. Therefore, the losses due to the magnetic and electric fields in the core, i.e., the iron loss P is obtained by summing (8)–(10) when the core sizes (R, l), the medium parameters (σ, μ, ϵ), and the exciting condition H_R are given:

$$P = P_M + P_E + P_D. \quad (11)$$

III. Consideration of the Dynamic Magnetic Loss

A. Iron Loss Evaluation by Fundamental Analysis

We measured the frequency characteristics of the iron loss obtained from two different size toroidal cores made

TABLE I
DIMENSIONS OF THE FERRITE TOROIDAL CORES (mm)

	Inside diameter	Outside diameter	Height
Small	6	12	3
Large	52	72	10

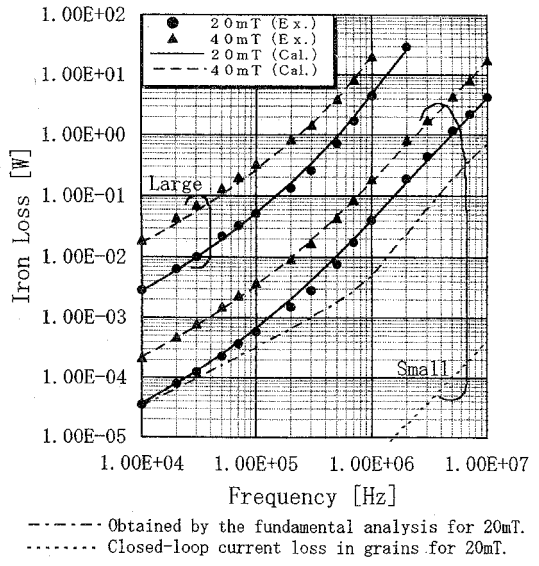

Fig. 2. Frequency characteristics of the iron loss for $B_m = 0.02$ [T] (●), $B_m = 0.04$ [T] (▲), and calculated losses (shown by the lines) for the large and small cores for which sizes are given in Table I.

of the same Mn–Zn ferrite whose μ and σ are comparatively low among Mn–Zn ferrite materials. In the previous section, we assumed that the toroidal core has a circular cross section. However, the toroidal cores used in the experiments have square cross sections and the dimensions listed in Table I. The measured frequency characteristics of the iron loss are depicted by the solid circles and triangles in Fig. 2. We measured two exciting conditions expressed by the maximum magnetic flux density B_m (0.02 and 0.04 T) which corresponds to the average of $\sqrt{2}B(r)$ in the cross section shown in Fig. 1. The experiments are carried out by using a prototype B–H analyzer (HP Ltd.) which computes the iron loss with the exciting current and the voltage induced in a search coil. B_m is computed from the voltage of the search coil, and is fixed to the specified values by controlling the amplitude of the exciting voltage automatically in the measurement system. In Fig. 2, we expressed the iron loss by [W] instead of the commonly used [W/m^3] (its volume density) so as to describe the iron loss characteristics of the different size cores in the same figure and to avoid the misunderstanding that the iron loss distributions are uniform in the cores.

In this section, we focus our attention on the measured points (●) of $B_m = 0.02$ [T] for the small core shown in Fig. 2. In order to analyze these iron losses by considering 2), 3), and 4) in the previous section, we need the medium parameters σ, μ, and ϵ of the ferrite used in the experiments. Let us discuss how to obtain μ, σ, and ϵ. Fig. 3 shows the frequency characteristics of iron loss density in one period of the excitation [J/m^3] on the condition $B_m = 0.02$ [T]. From Fig. 3, it is observed that the iron losses under 10 kHz appear independent of the exciting frequency. Therefore, these iron losses can be regarded as only the dc magnetic hysteresis loss. The iron loss measurement at 1 kHz gives the complex permeability

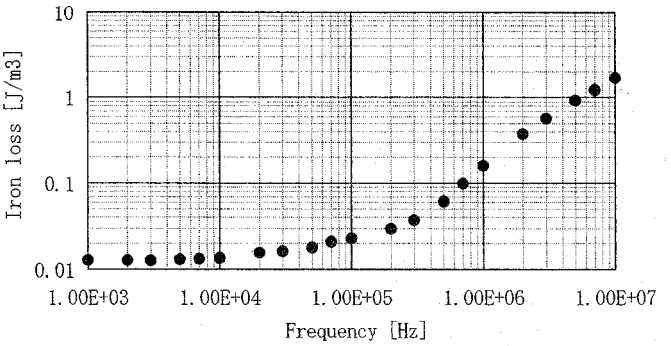

Fig. 3. Iron loss density per period in the small core on $B_m = 0.02$ [T].

$$\mu = \mu' - j\mu'' = (3080 - j122)\mu_0 \tag{12}$$

with the permeability of a vacuum μ_0. In this section, we use this value of μ in order to take the dc magnetic hysteresis loss into account. The application of a dc voltage to a core body made of the same ferrite as used in this paper gave a dc conductivity σ of 0.1 S/m, which is the same as its nominal value [10]. The relative permittivity $\epsilon_r = 100\,000$ of the ferrite was obtained by applying ac voltages from 100 Hz to 1 MHz to the same core body [10]. Assuming that the displacement currents in grain boundary regions flow into grains in series gives the formulation

$$E = \frac{1}{\epsilon_0\epsilon_r} D + j\frac{\omega}{g} D \tag{13}$$

where ϵ_0 denotes the permittivity in a vacuum and g [S/m] is an equivalent conductivity for the displacement currents. The value of g is obtained by applying a high-frequency voltage of more than 10 MHz to the core body because grain boundary regions are assumed to be short-circuited or purely resistive. According to the experiments carried out in [10] on this condition, we have $g = 10$ [S/m] for the same ferrite. Therefore, the complex permittivity ϵ is obtained from (13) and $D = \epsilon E$ as follows:

$$\epsilon = \epsilon' - j\epsilon'' \tag{14}$$

where

$$\epsilon' = \frac{\epsilon_0\epsilon_r g^2}{\omega^2(\epsilon_0\epsilon_r)^2 + g^2} \tag{15a}$$

$$\epsilon'' = \frac{\omega(\epsilon_0\epsilon_r)^2 g}{\omega^2(\epsilon_0\epsilon_r)^2 + g^2}. \tag{15b}$$

Applying the medium parameters σ, μ, and ϵ to (8), (9), and (10), respectively, gives the frequency characteristics of the iron loss (11), described by a chained line in Fig. 2. In these iron loss calculations, we made the area of the circular cross-section shown in Fig. 1 equal to the square area obtained from the small core dimensions listed in Table I. It is observed from the chained line that the iron loss increases rapidly from about 1 MHz because the dielectric loss occurs in addition to the dc magnetic hysteresis loss. However, the computational results are smaller than the experimental ones (●), particularly in a high-frequency range.

In the analysis above, we assumed a medium-homogeneous field represented by σ, μ, and ϵ, and ignored eddy currents circulating inside grains. Assuming that the grains are spheres having diameter d and conductivity κ (we assume κ is larger than g here), the eddy current loss density caused by these closed-loop currents in the grains is given by [1]

$$P_{EG} = \frac{\kappa(d\omega B_m/2)^2}{20} \text{ [W/m}^3\text{]}. \tag{16}$$

Calculating p_{EG} with $d = 20$ [μm] and $\kappa = 200$ [S/m], which is assumed to be the conductivity of an Mn–Zn single crystal [12], we show a dotted line in Fig. 2 for the small core on the condition $B_m = 0.02$ [T]. In spite of using the maximum possible values of d and κ, the computed losses are negligibly small compared to the experimental results. Therefore, we carry out our analyses with the assumption of the medium-homogeneous field in the following sections.

B. Introduction of a Dynamic Magnetic Loss Parameter

With two different size cores made of the same ferrite, we discuss in this section whether the iron loss remainders (the residual loss) obtained by subtracting the computational values from the experimental results are caused by the magnetic field in the z direction or by the electric field in the θ direction.

First, in addition to the losses considered in Section III-A, we assume a dynamic magnetic loss which increases in proportion to the square of the exciting frequency. In general, the dynamic magnetic loss is assumed to increase in proportion to the square of dB/dt. From this assumption, the magnetic field intensity is written by

$$H = \frac{1}{\mu_0\mu_r} B + j\frac{\omega_0}{\lambda_{h0}} B + j\frac{\omega}{\lambda_f} B \tag{17}$$

with the relative permeability μ_r of the ferrite. In (17), λ_{h0} [Ω/m] is called the hysteresis parameter [6] obtained from the complex permeability at the angular frequency ω_0 where the dc magnetic hysteresis loss is dominant in the iron loss and λ_f [Ω/m] is a newly introduced parameter (*the dynamic magnetic loss parameter*) in this paper to express the dynamic magnetic loss. In previous studies [3]–[5], the magnetic field intensity was decomposed into the in-phase and orthogonal components to the magnetic flux density in the time coordinate, which is similar to (17). However, the dc magnetic hysteresis loss and the dynamic magnetic loss were mixed and treated together by using a nonlinear parameter, or the eddy current loss was expressed by the $j\omega B$ term for convenience in addition to the magnetic losses. In contrast, (17), which concerns only the magnetic losses, treats the dc magnetic hysteresis loss and the dynamic magnetic loss separately with λ_{h0} and λ_f where λ_{h0}/ω_0 and λ_f are independent of the frequency. At 1 kHz, the third term on the right-hand side of (17) is negligible, so that μ_r and λ_{h0} are given with (12) and $B = \mu H$ as follows:

TABLE II
PARAMETERS FOR ANALYZING THE IRON LOSS (1)

B_m [T]	μ_r	λ_{h0} [Ω/m] (1 kHz)
0.02	3080	615
0.04	3080	400

$$\mu_r = \frac{\mu' + \mu''^2/\mu'}{\mu_0} \tag{18}$$

$$\lambda_{h0} = \omega_0(\mu'' + \mu'^2/\mu''). \tag{19}$$

From (12), we have $\mu_r = 3080$ and $\lambda_{h0} = 615$ [Ω/m] for $B_m = 0.02$ [T], as listed in Table II where λ_{h0} is obtained at $\omega_0 = 2\pi \times 1000$ [rad/s]. In order to combine the imaginary terms of (17) by $j\omega$, we introduce

$$\lambda_h = \lambda_{h0}\frac{\omega}{\omega_0} \tag{20}$$

and

$$\lambda = \frac{\lambda_h\lambda_f}{\lambda_h + \lambda_f}. \tag{21}$$

With (20) and (21), μ' and μ'' are written by

$$\mu' = \frac{\mu_0\mu_r\lambda^2}{\omega^2(\mu_0\mu_r)^2 + \lambda^2} \tag{22a}$$

$$\mu'' = \frac{\omega(\mu_0\mu_r)^2\lambda}{\omega^2(\mu_0\mu_r)^2 + \lambda^2}. \tag{22b}$$

Substituting $\lambda_f = 57 \times 10^3$ [Ω/m] into (21) gives the frequency characteristics of the iron loss, described by the solid ($B_m = 0.02$ [T]) and broken ($B_m = 0.04$ [T]) lines in Fig. 2 for the small and large cores. In these computations, we used the same values of σ, ϵ_r, and g as the chained line of Fig. 2, as shown in Table III. In the case of $B_m = 0.04$ [T], we substituted $\lambda_{h0} = 400$ [Ω/m] (Table II), obtained by the complex permeability at 1 kHz, into (20) because the dc magnetic hysteresis loss depends on B_m. If we apply λ_f larger than 57×10^3 Ω/m to the analysis, computed results become smaller than the measured values. For example, in the case of the small core on the condition $B_m = 0.02$ [T], the computed curve approaches

TABLE III
PARAMETERS FOR ANALYZING THE IRON LOSS (2)

	B_m[T]	λ_f[Ω/m]	σ[S/m]	ε_r	g[S/m]
——·——·——	0.02	∞	0.1	100000	10
————	0.02	57000	0.1	100000	10
- - - - - -	0.04	57000	0.1	100000	10
——··——·——	0.02	∞	50	100000	10
·····	0.02	57000	0.1	$\varepsilon=0$	

the chained line of Fig. 2 when we increase λ_f up to infinity. On the other hand, decreasing λ_f gives iron losses larger than the measured values. Therefore, the iron loss difference (the residual loss) shown in Section III-A can be explained by introducing the third term on the right-hand side of (17), regardless of core size.

Secondly, let us discuss the possibility that the residual loss is caused by the electric fields in the θ direction. In this case, we have two possibilities for the iron loss increase: the eddy current loss due to σ and the equivalent dielectric loss. We attempt to determine the value of the medium parameter σ or g which adapts the computational iron losses to the measured ones. In the analysis here, we assume that λ_f is infinite in order to remove the effect of the dynamic magnetic loss term. We varied the value of g at 1 MHz for the small core with $\sigma = 0.1$ [S/m], $\epsilon_r = 100\,000$, and $B_m = 0.02$ [T]. We obtained the maximum iron loss at $g = 6.0$ [S/m]; however, its value was only 13% of the measured iron loss, and thus could not account for the residual loss shown in Section III-A. In a similar analysis of the ohmic loss increase due to σ, given $\epsilon_r = 100\,000$, $g = 10$ [S/m], and $B_m = 0.02$ [T], $\sigma = 50$ [S/m] gives the computational iron loss curves depicted by the chained lines (Table III) in Fig. 4 for the small and large cores. This value of σ is almost suitable for the small core; however, it cannot shed light on the experimental iron loss curve for the large core.

From the discussion above, we conclude that the residual loss is the dynamic magnetic loss. In addition, it is revealed from a comparison of the chained and solid lines (Table III) for the small core, shown in Fig. 2, that the dynamic magnetic loss becomes dominant in a high-frequency region. We notice that the magnetic flux density distribution in a high-frequency range affects the hysteresis parameter λ_{h0} at each position because λ_{h0} depends on the amplitude of the magnetic flux density. However, the dc magnetic hysteresis loss hardly reflects the iron loss quantitatively in the high-frequency region. Therefore, the computed iron loss error due to λ_{h0} fluctuation is negligible.

C. Damping Coefficient of Magnetic Domain Wall Motion

The magnetic domain wall structure of ferrites is different from that of the metallic materials. However, from

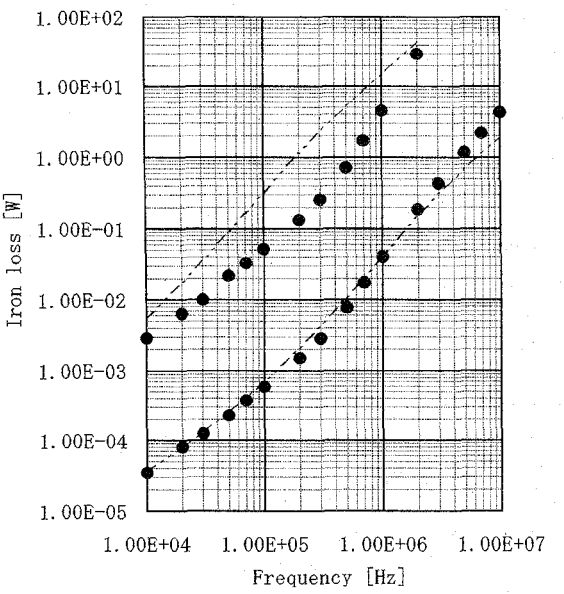

Fig. 4. Computed iron loss curves obtained by assuming $\sigma = 50$ [S/m] (chained lines) and comparing them to the experimental results (●).

a macroscopic point of view, we can analyze the velocity and damping coefficient of the magnetic domain wall motion in ferrites. If we assume one domain wall and its velocity [m/s] in a core cross section, we lose the consistency of the analysis because the dumping coefficient of the velocity depends on a supposed wall motion trajectory or the length of the wall, even if the cross-sectional area is the same. This is because the velocity depends on the wall length at the same exciting frequency. It is more comprehensible when we have a core whose cross section is rectangular and assume domain walls facing different directions. Hence, we assume multiple domain walls and the areal velocity ν [m^2/s] on the cross section as the sum of their movements. Then, we have the damping coefficient β [A · s/m^3] by arranging the product of β and ν to have the dimension of the magnetic field intensity [A/m]. Supposing a low frequency at which the magnetic field is uniform in the core shown in Fig. 1, the total magnetic flux Φ is given by

$$\Phi = B\pi R^2. \tag{23}$$

Let B_s denote the saturation induction; we have the time derivative of Φ:

$$\omega\Phi = 2B_s\nu \tag{24}$$

where ν is expressed by the effective value. With (23) and (24), the loss density p_f [W/m^3] owing to the domain wall motion is written by

$$p_f = (\beta\nu)\cdot(\omega B) = \frac{2B_s\beta}{\pi R^2}\nu^2 \tag{25}$$

because $\beta\nu$ is the magnetic field intensity yielding p_f. From (23) and (24), the areal velocity ν is obtained by

$$\nu = \frac{\pi R^2\omega B}{2B_s}. \tag{26}$$

TABLE IV
DAMPING COEFFICIENTS FOR THE DOMAIN WALL MOTION

	β[As/m^3]	β'[Js/m^5 or Ns/m^4]
Small	2.0	2.0
Large	0.18	0.18

The magnetic field intensity expressed by the third term on the right-hand side of (17) yields the dynamic magnetic loss which corresponds to p_f because it increases in proportion to the square of the exciting frequency, i.e.,

$$p_f = \left(\frac{\omega}{\lambda_f} B\right) \cdot (\omega B) = \frac{\omega^2}{\lambda_f} B^2. \tag{27}$$

Therefore, we obtain β from (25) and (27), or by letting the magnetic field intensity $\beta v = \omega B/\lambda_f$:

$$\beta = \frac{2B_s}{\lambda_f \pi R^2}. \tag{28}$$

It is found from (28) that the damping coefficient β depends not only on the dynamic magnetic loss parameter λ_f, but also on πR^2, i.e., the cross-sectional area of the magnetic flux path in a core. When we compose the equation of the magnetic domain wall motion, having the dimension [J/m^3] or [N/m^2] instead of [A/m], the damping coefficient β' [Js/m^5] or [Ns/m^4] is given by

$$\beta' = 2B_s\beta \tag{29}$$

which is still a function of the cross-sectional area of a core. The nominal value of B_s of the ferrite used in this study is 0.51 T at 25°C. With this value, we computed β' for the small and large cores, and listed them with β in Table IV.

IV. IRON LOSS DENSITY DEPENDENCE ON CORE DIMENSIONS

In previous studies [7], [11], it was reported that the frequency characteristics of the iron loss in ferrites depend on core dimensions, even if the cores are made of the same ferrite. In other words, the average iron loss density depends on core dimensions subject to the same exciting frequency and B_m. In the case of metallic materials, it is explained by the difference of the eddy current distribution in cores. However, ferrites have very low conductivities compared to the metallic materials, so that we find here, with the small and large cores, how much the displacement currents in ferrite cores affect the iron loss dependence on core dimensions. The dotted lines of Fig. 5 show the computational results (B_m = 0.02 [T]) obtained when we neglect the displacement currents in the cores by substituting $\epsilon = 0$ into the governing equations (1) and (2). For comparison, the experimental results of

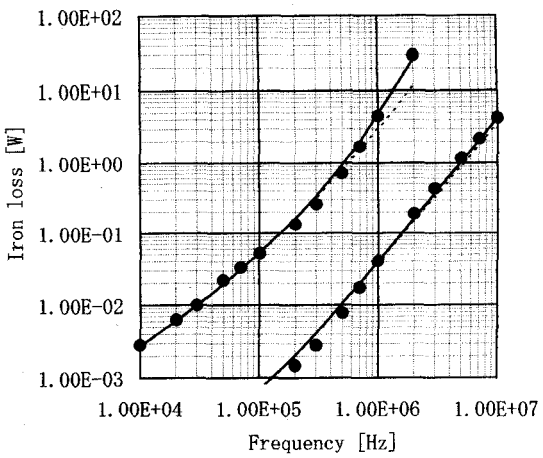

Fig. 5. Influence of the displacement currents on the iron loss. The dotted lines show the computed results obtained by neglecting the displacement currents.

TABLE V
PERCENTAGE EVALUATION OF P_M, P_D, AND P_E

	Large (2MHz)	Small (2MHz)	Small (10MHz)
P_M[%]	55.6	90.1	85.1
P_D[%]	43.6	9.7	14.8
P_E[%]	0.8	0.2	0.1

B_m = 0.02 [T] are also shown in the same figure, in addition to the computational results described by the solid lines in Fig. 2. The dotted lines are obtained under the same condition of the medium parameters as the solid lines, except for $\epsilon = 0$ (Table III). From Fig. 5, it is found that the displacement currents considerably affect the iron loss of the large core in the megahertz range, while this effect is little in the small core. In order to investigate in detail, the percentages of P_M, P_D, and P_E with respect to P at three representative points on the solid lines are listed in Table V. The equivalent dielectric loss P_D due to the displacement currents occupies more than 40% at 2 MHz in the large core, while it is under 10% in the small core under the same condition. The small core has only about 15% dielectric loss, even at 10 MHz. In every case, the percentage of the eddy current loss P_E owing to σ is less than 1%. From the discussion above, it is clarified that the iron loss dependence on core dimensions is caused by the displacement currents, i.e., the large permittivity of ferrites. In other words, a large cross section of the magnetic flux path facilitates the magnetic flux to have a skin effect due to the displacement currents. However, it is obvious that the magnetic flux and displacement current distributions are independent of the magnetic flux path length.

V. CONCLUSIONS

In this study, the iron loss measurements of two different size cores of the same Mn–Zn ferrite material were

carried out up to the megahertz range, and the iron loss at each frequency was analyzed by taking into account the magnetic and electric field distributions in the cores. In the analysis, we considered the ohmic losses in grains, owing to the displacement currents in grain boundary regions, as the equivalent dielectric loss by using complex permittivity. Examining the measured frequency characteristics of the iron loss with the computations, including some tentative simulations, leads to the following conclusions.

1) The fundamental analysis only taking into account the dc magnetic hysteresis loss, the eddy current loss, and the ohmic loss due to the displacement current could not explain the measured frequency characteristics of the iron loss.

2) Introducing the dynamic magnetic loss parameter λ_f to the fundamental analysis provides reasonable iron loss characteristics consistent with the experimental results, independent of the core size and exciting conditions.

3) The dynamic magnetic loss becomes dominant in a high-frequency region, and it corresponds to the one called the residual loss of ferrites in the past.

4) The damping coefficient of magnetic domain wall motion β is expressed by λ_f. Also, β is a function of the cross-sectional area of a magnetic flux path.

5) In ferrites, the dependence of iron loss density on core dimensions is caused by the difference in displacement current distribution, and a large cross-sectional area of a ferrite core enhances the skin effect.

6) In this paper, we used a relatively low-μ and low-σ material among Mn–Zn ferrites. However, in the case of high-μ and high-σ Mn-Zn ferrites, it is predicted from this study that the dependence of iron loss density on core dimensions increases because grain boundary regions are thin, i.e., the displacement currents increase owing to large permittivity; in addition, the eddy currents increase due to high-σ.

7) For future ferrite materials used in a high-frequency region, it is expected that the dynamic magnetic loss should be reduced rather than decreasing the conductivity σ further. Moreover, decreasing the permittivity for large cores is effective in reducing the iron loss.

The frictional loss of domain wall motion can be evaluated by using the dynamic magnetic loss parameter λ_f, which will help us find a clue to clarify the mechanism of generating the dynamic magnetic loss.

ACKNOWLEDGMENT

The authors would like to thank T. Tadano of TDK Corporation for providing the Mn–Zn ferrite cores used for this study.

REFERENCES

[1] R. M. Bozorth, *Ferromagnetism.* Princeton, NJ: Van Nostrand, 1951, pp. 778–779.

[2] R. H. Pry and C. P. Bean, "Calculation of the energy loss in magnetic sheet materials using a domain model," *J. Appl. Phys.*, vol. 29, pp. 532–533, Mar. 1958.

[3] Y. Saito, "Three-dimensional analysis of magnetodynamic fields in electromagnetic devices taken into account the dynamic hysteresis loops," *IEEE Trans. Magn.*, vol. MAG-18, pp. 546–551, Mar. 1982.

[4] Y. Saito, H. Saotome, S. Hayano, and T. Yamamura, "Modeling of nonlinear inductor exhibiting hysteresis loops and its application to the single phase parallel inverters," *IEEE Trans. Magn.*, vol. MAG-19, pp. 2189–2191, Sept. 1983.

[5] S. Hayano, H. Saotome, A. Miyazaki, and Y. Saito, "A representation of magnetization characteristics for computational magnetodynamics," *Int. J. Appl. Electromagn. Mater.*, vol. 2, pp. 353–358, 1992.

[6] T. Sato and Y. Sakaki, "Physical meaning of equivalent loss resistance of magnetic cores," *IEEE Trans. Magn.*, vol. 26, pp. 2894–2897, Sept. 1990.

[7] Y. Sakaki and T. Sato, "Large signal eddy current losses beyond 100 kHz," *IEEE Trans. Magn.*, vol. MAG-20, pp. 1487–1489, Sept. 1984.

[8] J. Smit and H. P. J. Wijn, *Ferrites.* Eindhoven, The Netherlands: Philips Research Laboratories N.V. Philips' Gloeilampenfabrieken Eindwoven, 1959, pp. 236–241.

[9] K. J. Standley, *Oxide Magnetic Materials.* Oxford: Clarendon, 1972, pp. 140–143.

[10] Y. Sakaki, M. Yoshida, and T. Sato, "Formula for dynamic power loss in ferrite cores taking into account displacement current," *IEEE Trans. Magn.*, vol. 29, pp. 3517–3519, Nov. 1993.

[11] T. Matsuoka, T. Sato, and Y. Sakaki, "Dimension dependence of power losses in polycrystalline Mn–Zn ferrite cores" (in Japanese), *IEICE Trans.*, vol. J71-C, pp. 1128–1133, Aug. 1988.

[12] T. Sato and Y. Sakaki, "Mechanism generating power losses in MHz band in polycrystalline Mn–Zn ferrite cores used for switching power supplies" (in Japanese), *IEICE Trans.*, vol. J71-C, pp. 1121–1127, Aug. 1988.

Hideo Saotome (M'96) was born in Tokyo, Japan, on December 13, 1958. He received the B.E. and M.E. degrees in electrical engineering from Hosei University, Tokyo, in 1981 and 1983, respectively. In 1981 he was a visiting postgraduate student at McGill University, Montreal, Canada. He received the Ph.D. degree in inverse problem analysis from Hosei University in 1994.

In 1983 he joined Fuji Electric Corporation Research and Development, Ltd., and was engaged in research on power electronics. In 1993 he was with the Laboratoire d'Electrotechnique de Grenoble, France, as a Research Fellow. He is presently an Associate Professor in the Faculty of Engineering, Chiba University, Chiba, Japan.

Dr. Saotome is a member of IEE Japan and the Magnetics Society of Japan.

Yo Sakaki (M'83) was born in Chiba, Japan, on March 9, 1932. He received the B.S. degree in electrical engineering from Ibaraki University in 1954, and the M.Eng. and D.Eng. degrees from Tohoku University 1965 and 1971, respectively.

From 1954 to 1963 he was engaged in the research and design of magnetic amplifiers and power semiconductor devices for several companies. In 1969 he joined the Faculty of Engineering, Chiba University, Chiba, Japan, where he is presently a Professor. His current research interests include the mechanism generating power loss in soft magnetic materials including ferrite, the biomagnetic sensor in migratory fish, and the application of nonlinear magnetic devices.

Dr. Sakaki is a member of IEE Japan, IEICE Japan, and the Magnetics Society of Japan. From 1991 to 1993 he was Chairman of the IEEE Magnetics Chapter, Tokyo Section. Since 1993 he has been chairman of the Technical Group on Magnetics of IEE Japan.